Research Article

Nano Biomed Eng

Antibacterial Activity and Optical Behavior for Restoration of Micro and Nano Dental Fillers Using Functional Graphene Nanosheets with Polymethyl Methacrylate

Abbas Kadhim Hassan[1,2], Habib Hamidinezhad[1], Ehssan Al-Bermany[3]

[1] Department of Physics, Faculty of Basic Sciences, University of Mazandaran, Babolsar 48175-866, Iran
[2] Educational Directorate of Babylon, Ministry of Education, Bagdad 10069 Iraq
[3] Department of Physics, College of Education for Pure Sciences, University of Babylon, Babil 51002, Iraq

Corresponding author. E-mail: ehssan@uobabaylon.edu.iq

Received: Oct. 4, 2023; **Revised:** Dec. 4, 2023; **Accepted:** Dec. 15, 2023

Citation: A.K. Hassan, H. Hamidinezhad, E. Al-Bermany. Antibacterial activity and optical behavior for restoration of micro and nano dental fillers using functional graphene nanosheets with polymethyl methacrylate. *Nano Biomedicine and Engineering*, 2024, 16(4): 652−664.
http://doi.org/10.26599/NBE.2024.9290075

Abstract

Polymer-based graphene nanocomposites significantly impact dental filler materials and antibacterial applications. Polymethyl methacrylate (PMMA) was used to improve the properties of nano and hybrid-dental fillings reinforced using synthesis graphene oxide (GO). Developed acoustic-solution-sonication-casting procedures were used to fabricate the new PMMA-dental filler-GO nanocomposites and the morphology, structure, optical properties, and antibacterial activity of samples were investigated. Fourier transforms infrared (FTIR) exposed good interaction among the PMMA, filling, and GO nanosheets. Scanning electron microscopy (SEM) and optical microscope (OPM) images revealed homogeneous samples and fine dispersion with improved morphology and overcoming cavities and cracks in the samples. The incorporation of PMMA and PMMA-GO in the nanocomposites showed promising properties: Absorption peak presented at 320 nm of samples enhanced from 0.8 (N1) to 0.98 (N3) for nano-fillers and from 0.7 (H1) to 0.97 (H3) for hybrid-fillers. Bandgap reduction from 3.35 (N1) to 3.15 (N3) for nano-fillers and from 3.10 (H1) to 2.75 (H3) for hybrid-fillers in allowed indirect transition, whereas it reduced from 3.38 (N1) to 3.00 (N3) for nano-fillers and from 3.05 (H1) to 2.75 (H3) for hybrid-fillers in forbidden indirect transition after the contribution of PMMA and GO nanosheets. The inhibition zone of the *Klebsiella* bacteria significantly expanded from 17 to 23 mm for nano-fillers and from 16 to 22 mm for hybrid-fillers. Nanofillers nanocomposites presented better properties and inhabitances zone diameter of antibacterial compared with non-reinforced dental fillers.

Keywords: antibacterial; dental fillers; grapheme; *Klebsiella*; nanocomposites; optical properties; polymethyl methacrylate (PMMA)

Introduction

Polymer-composites-based resin is the most popular material in dental restorations because of its superior aesthetic quality, mechanical properties, etc. Moreover, the additive utilized to restorative the dental could adhere to the hard tissues of the teeth, allowing for a non-invasive caries removal technique

[1, 2]. Despite these benefits, polymeric composites have some disadvantages, for instance, polymerization contraction with affinity for bacterial adhesion [3, 4]. In addition, micro-organisms exists between the dental restoration and healthy tissues have easy access to the regenerated dental tissues via microcavities at the tooth–restoration interface [5]. Many bacteria are responsible for diseases, including gingivitis, ulcers, and tooth decay [6]. Cavities form when bacteria in the mouth produce acid, eroding the tooth's cementum, dentin, and enamel. The decay of teeth is the result of this process [7, 8]. The primary cause of tooth restoration failure is caries at the margin of composite dental restorations [9].

In the past three decades, dental fillings have been extensively used for anterior and posterior restorations [10]. Unfortunately, research indicates that the secondary caries contributes significantly to the high failure rate. According to the research, plastic builds up faster on resin composites than enamel or traditional restorations [11]. Therefore, modifications incorporating antibacterial properties are necessary to expand the service life of resin composite restorations [12, 13]. In addition, composite dental filling materials have endured a series of qualitative and revolutionary advancements from the time they were first developed to the present. Due to the compound's complexity, these materials covered required good properties [14]. In addition, it cannot cause damage to the body, or release any toxic chemicals while in the mouth [15]. Furthermore, it should be antibacterial [16]. Moreover, this filler must meet various optical standards to show the appropriate view with natural teeth [17]. Thus, clinical, industrial, and researcher interest in developing, restoration, anticorrosion and antibiofilm adhesives using polymers, nanomaterials, or other materials has increased in recent years [18, 19].

Polymer is commonly utilized for dental bases, artificial teeth, cements, pigments, provisional crowns, endodontic fillings, and tissue conditioners, and other applications [20, 21]. A denture material must withstand the masticator burden over an extended period with minimal irritation [22]. The raw material is suitable and must not react with the mouth' s aqueous environment [13]. It must resist the cracking caused by solvents found in foods, beverages, and medications. Also it must be taken into consideration that the materials's sensitivity to changes in atmospheric conditions [23]. Its exceptional polymer properties, for instance, optical, mechanical, thermal, electrical, conditions resistance, and formability, make polymer an excellent candidate [24]. Since 1937, one of the best dental polymer candidates is polymethyl methacrylate (PMMA). It has become increasingly popular in recent years [25] and is one of the most appropriate polymers for dental applications, which is the focus of the current research. In addition to its advantageous mechanical, physical, and biological properties, it is simple to produce with low cost [26]. Furthermore PMMA is widely used in prostheses, bone cement, long-term fix materials, and other applications [27].

Recently, nanofillers were incorporated as components of dental fillers to overcome polymer-related problems [28]. Carbon materials and graphene oxide is among the most exciting nanomaterials utilized in dentistry today [29, 30]. The scientific community is interested in graphene, which is unique and applicable in various situations [31]. In the dental discipline, graphene and graphene-derived nanomaterials are gaining popularity, and their use in dentistry is necessary. These nanomaterials are evaluated to ensure that their biocompatibility [32]. Graphene-based materials can be adapted in novel applications through modifying their chemical and physical properties [33]. The distinctive and prospective characteristics of graphene include its abundant range of various functional groups, nano-sized sheets, capabilities with excellent conductivity, and mechanical and optical properties [34], and antibacterial properties [23].

Graphene-polymer nanocomposites significantly impact dental filler properties and antibacterial activity [1]. Bacali et al. [35] used graphene with silver to reinforce PMMA in denture wearers for photodynamic therapy that significantly inactivates halitosis-responsible bacteria in acrylic dentures. Graphene–silver nanoparticles with 1 wt.% and 2 wt.% loading ratios were added to a commercial acrylic resin powder. PMMA acrylic resins reinforced by 1 wt.% and 2 wt.% of graphene–silver nanoparticles exhibited antimicrobial impacts on halitosis-responsible bacteria, which improved the bacteria inhibition zone. That was significantly enhanced after applying laser light and with 2 wt.% concentrations of nanoparticles. Bregnocchi et al. [1] utilized different loading ratios of graphene-based materials to apply as fillers in the polymer dental

adhesives. The results showed biofilm growth on tissues of the adhesive-covered dentine that exhibited antiadhesion properties for dental product materials. Malik et al. [36] described a new, straightforward, and inexpensive method for producing a few layers from multi-layer commercial graphene and combining them into dental polymers as composites. The study showed considerable mechanical properties of graphene-dental polymer composites compared to the control group's dental polymer; the graphene-dental polymer enhanced compressive strength and compressive modulus by up to 27% and 22%, respectively. Aunkor et al. [37] demonstrated that graphene oxide has antibacterial activity and good biocompatibility as they tested GO against various life-threatening MDR superbugs, including *Escherichia coli*, *Pseudomonas aeruginosa*, *Klebsiella pneumoniae*, *Serratia marcescens*, *Proteus mirabilis*, and *Staphylococcus aureus*. The minimal inhibitory determination revealed the final effective concentration of the drug. Increasing concentration of GO inhibits the viability of these pathogens more effectively that it is accomplished by puncturing the cell's walls, dispersing the bacterial genome, and isolating the bacteria from the growth medium. Moreover, they compared the various ranges of bactericidal activity of GO, indicating it has the potential to be used as a new antibiotic. In 2020, Dhulfiqar et al. [38] utilized nano-graphene and nano-silica into resin composite for dental fillers. The relationship between topography and mechanical properties was studied. They used LED curing in the three periods (20–25–30) with the addition of the filler. The mildew finished in magnitudes of 6 mm × 3 mm. The results exhibited the impact of increasing the curing time is critical for optimizing the polymerization process. Whereas, mechanical characteristics analysis exposed nano graphene presents a higher compressive resistance than nano silica. Atomic force microscope (AFM) measurements show that nanographene's surface is rougher than nano-silica. Bacali et al. [35], used graphene–silver, PMMA, and photodynamic therapy to kill germs in people who wear dentures. The point of this study was to find out if it was possible to kill germs in acrylic dentures. A store-bought acrylic resin powder had 1 wt.% and 2 wt.% graphene silver nanoparticles added to it. When graphene silver nanoparticles were mixed with PMMA acrylic resins, they killed bacteria that cause bad breath. Using a photosensitizing agent on denture base materials that were enhanced with graphene silver nanoparticles (1 wt.% and 2 wt.%) also helped kill more bacteria which cause bad breath in people who wear acrylic dentures, especially when laser light and higher nanoparticle concentrations (2 wt.%) were used.

Several investigations have reported the improving properties of the dental filler, such as mechanism or life time. The mechanism, life time, optical behavior, and adsorption, such as the absorption behavior of materials that deals with different food, acids, sugar, etc. in addition to the growing of bacteria and decay of the dental materials are still not fully understood, and future studies need to focus on producing better materials. Therefore, the present study will help to reduce the gap and provide mor information in this field.

The study objective is to investigate the effect of PMMA and PMMA-GO on the optical properties and antibacterial activity of two dental fillings containing micro- and nano-scale materials. The PMMA and GO nanosheets modify and reinforce the filler's structure, optical properties, and antibacterial activity for dental materials. Various characterizations were used to characterize the samples, for instance, Fourier transform infrared (FTIR), oblique plane microscopy (OPM) images, scanning electron microscope (SEM), and ultraviolet–visible (UV–Vis) spectroscopy. The antibacterial activities, and the effectiveness of the PMMA-nano/hybrid dental filler-GO nanocomposites also were investigated thoroughly.

Experimental

Materials

The hybrid filler is known as BEAUTIFIL II (Bis-GMA). It is a macro–micro particle produced from bisphenol a-glycidyl methacrylate, trimethylene glycol dimethacrylate (5%), aluminofluoroborosilicate glass (60%–70%), aluminum oxide (5%), and DL-camphor quinone (1%) that produces as resin by Shofu Inc. company in Japan. Nano-hybrid universal material combines Bis-GMA and barium glass with nanosize silica (10–50 nm) and prepolymer purchased from Sincera Technology Company, China. PMMA has a molecular weight of 18 000–20 000 g/mol, a melting point of 213 ºC, and 99% purity produced by Tuttlingen Company in China. Our group synthesized

GO following the procedure from our previous publication [2] and modified Hummer methods [39]; it has a pH of ~ 5.7 (see the supplementary material for complete characterizations of GO nanosheets). Dimethylformamide (DMF) (C_3H_7NO) with molar mass 73.09 g/mol, minimum assay 99% was used as a solvent manufactured by Thomas Baker (MIDC), Chemical Zone, India.

Fabricated filler-polymer-based graphene nanocomposites

Developed aquatic dissolving-sonication-casting procedures were applied to produce new modified PMMA-nano/hybrid dentil filler-GO nanocomposites. Three samples were fabricated for each filler. Briefly, at (80 ± 2) ºC PMMA was dissolved in DMF for 3 h independently. Firstly nano/hybrid fillings were fully dissolved independently in DMF for 3 h, to prepare the reference samples. Secondly, PMMA-DMF was mixed with dissolved nano/hybrid-DMF filling samples independently for each sample to prepare PMMA-nano/hybrid filler samples. That was mixed with a ratio of 25:75 (w/w) of PMMA:nano-filler and PMMA:hybrid filler for 3 h to prepare the second samples of both fillers.Thirdly, GO was also dispersed in DMF with sonication for 30 min using a sonication bath to achieve complete dispersion in nanomaterials. GO-DMF was loaded to modify and reinforce the PMMA-nano/hybrid filler matrix structure with a ratio of 24:75:1 (w/w) of PMMA:nano/hybrid filler:GO. The PMMA-nano/hybrid filler-GO nanocomposite were mixed for 60 min. Matrix was sonicated for 10 min using a sonication bath. This procedure was repeated for 48 h until a homogeneous mixture of the PMMA-nano/hybrid filler-GO dental nanocomposites was achieved. A magnetic stirrer hot plate produced by Stuart company was used during all processes. Finally, the samples were washed with tepid distilled water to remove potentially harmful substances, centrifuged to collect the sediment materials, and cast in a Petri dish to dry at room temperature until thoroughly dried and the sample's thickness is between 0.6 and 0.9 μm. The fabricated samples were pure nano/hybrid filling, PMMA-nano/hybrid filling, and PMMA-nano/hybrid filling-GO nanocomposites, as summarized in Table 1 and the diagram in Fig. 1.

Characterizations

The FTIR spectra were measured using the Vertex 70 (Bruker Company, Germany) at the wavelength of 500–4 000 cm^{-1}. The surface morphology of the samples was captured using SEM (Mira-3, manufactured by Tescan, France, using the set of 1.2 nm at 30 kV and 2.3 nm at 3 kV), and X-ray diffraction (XRD) (Model Xpert, Tescan, France). Nikon 73346 OPM manufactured by Olympus Company (Japan), recorded the optical images. Shimadzu UV-1650 spectrophotometer product by Phillips company (Japan), was used in the wavelength range of 200–1 100 nm.

Results and Discussion

FTIR spectra are illustrated in Fig. 1 for nano/hybrid dental fillers and the nanocomposite samples. Nano

Table 1 The synthesis for the filler samples with nanocomposites

Sample ID	Filler type	Concentration (wt.%)		
		PMMA	Filler	GO
N1	Nano	00	100	00
N2	Nano	25	75	00
N3	Nano	24	75	1.0
H1	Hybrid	00	100	00
H2	Hybrid	25	75	00
H3	Hybrid	24	75	1.0

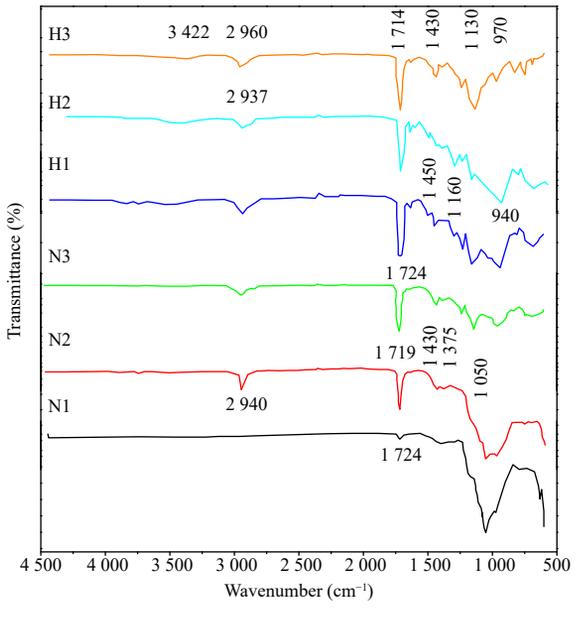

Fig. 1 FTIR spectra for samples: the pure dental filling (N1), nano filling-PMMA (N2), nano filling-PMMA-GO (N3), hybrid (H1), hybrid-PMMA (H2),and hybrid-PMMA-GO (H3).

filler (N1) curve revealed a small peak at 1 056 cm^{-1} related to C–O stretching, whereas new peaks presented in the N2 after the addition of the PMMA that showed a small peak at 1 726 cm^{-1} correlated to C=O stretching and shift in the peak at 1 056–1 055 cm^{-1} [40]. GO contribution in the PMMA-nano dental filler (N3), presented a new C–H medium stretching peak at 2 950 cm^{-1} and a peak at 1 239 cm^{-1} related to C–H stretching. The single bond C–C presented a medium absorption, respectively, in agreement with the result in Ref. [41]: it presented a shift in some of the peaks, such as from 1 726 to 1 723 cm^{-1} and from 1 055 to 1 045 cm^{-1}.

H1 curve displayed a small peak in 1 715 and 940 cm^{-1} associated with C=O stretching and C=C bending. H2 spectra show new peaks at 2 955, 1 431, and 1 145 cm^{-1} linked to C–H stretching. The C–C bond exhibits low vibration, whereas C–O is associated with ether group. Also, H2 revealed shifting in some peaks, for instance, from 1 715 to 1 720 cm^{-1} and from 940 to 950 cm^{-1}. GO influence in the PMMA-hybrid dental (H3) resulted in a new C–H stretching peak at 1 240 cm^{-1}. Furthermore, it depicted a shifting in some other peaks, for instance, from 1 720 to 1 724 cm^{-1} and from 1 140 to 1 170 cm^{-1}. The shifting, new peaks, and changes in intensity peaks of the FTIR spectra reflected the type of interactions between the components of the matrix, which is presented as strong interfacial interaction that could be mostly hydrogen bonds between additive materials with dental fillers [2, 40].

The images of the OPM of samples are exposed in Fig. 2 with 100× magnification. These pictures showed acceptable uniformity of dissolved N1 and H1 samples with smooth surfaces. The surface of the N2 and H2 matrix samples was observed presenting the dendrimers and branches after loading 25 wt.% PMMA that could create a unique network between the PMMA and dental materials. These dendrimers presented wider, bigger, and more dispersed amorphous of H2 compared with N1. Whereas the addition of GO nanosheets strongly impacted N3, the dendrimers could prevent or restrict it. Meanwhile, the N3 and H3 showed greater consistency and organization of dendrimers as trees with uniform size and shape. Changing the nanomaterial surface could correlate to the strongest hydrogen bonds that formed among the PMMA, dental fillers, and GO nanosheets, as shown in the FTIR spectra.

Figure 3 represents the sample surface morphology using SEM images. Two different magnifications were set of images at the μm scale, and then part of this image was magnified to 200 nm for each sample, as shown in Fig. 3. N1 revealed the composition as gritty particles, rough and cavities fracture surface. The nano-filling is illustrated in the image that can be found in Figs. 3(a). Whereas the morphology behavior was significantly altered, and the most-grained partials were covered in Figs. 3(b); additionally, to fill the cavities and spaces between the filler partials components, the nano filler-PMMA sample showed tiny cracks on the surface, which were related to the PMMA nature, as reported by another researcher [32]. This was the case even though the filler-PMMA sample filled the cavities and spaces between the filler partials components. These fissures were blocked, and the surface was strongly modified following the contribution of GO nanosheets, as shown in Figs. 3(c), due to the excellent interaction that occurred because of continuous mixing between the two components.

The surface topography of the hybrid filling sample (H1) was represented in Figs. 3(d), which showed gritty microparticles and rough and cavity fracture

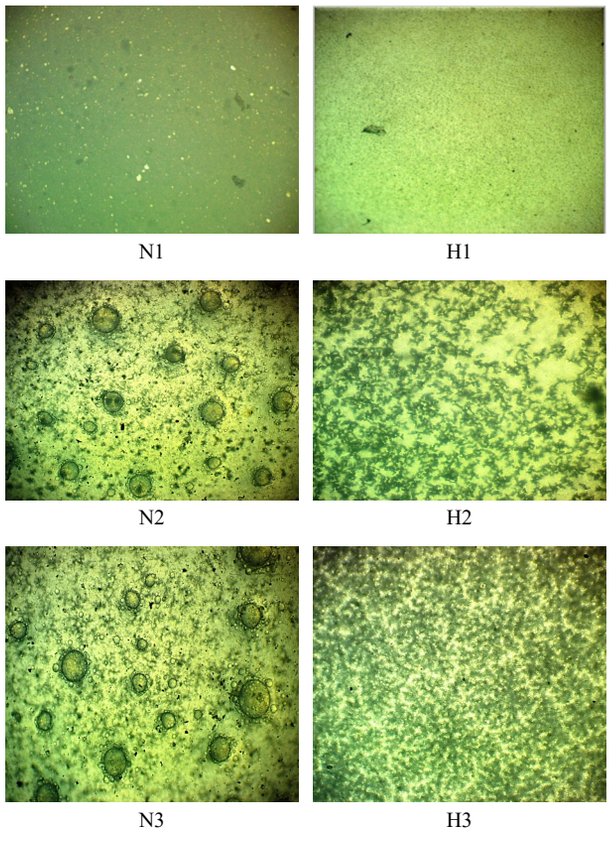

Fig. 2 OPM images of samples.

surfaces. Loading PMMA in the H2 sample covered most microparticles, filling the gaps and cavities among the filler matrix components. Moreover, the H2 surface exposed small fissures or cracks related to the natural PMMA surface, as resolved in Figs. 3(e). Meanwhile, GO significantly impacted the creation of several interfacial interactions and bonds between the component's materials. GO is associated with connecting the molecules closely to one another as networks with the help of dendrimers and branches already presented to crated complex connections that overcome the cracks and surface fissures, as presented in Figs. 3(f).

The morphology samples changed due to several factors, including long polymer chains that covered the most particles and cavities in the dental materials and bonded the filler matrix. Meanwhile, GO functional groups can form a more vital interfacial interaction among polymer, fillers, and GO. This is strongly exhibited in the FTIR spectra in agreement with Ref. [40].

The absorbance spectra for the pure dental filling (N1), nano filling-PMMA (N2), nano filling-PMMA-GO (N3), hybrid (H1), hybrid-PMMA (H2), and hybrid-PMMA-GO (H3) nanocomposite in the range 320–1 100 nm^{-1} wavelength are shown in Figs. 4 and 5. These figures show the absorption variance with wavelength for N1, N2, N3, H1, H2 and H3. Generally, the absorbance of samples revealed a high value in the electromagnetic spectrum ultraviolet region at 320 nm^{-1}. At the same time, the absorbance reduced gradually after increasing the wavelength to 1 100 nm^{-1}.

The absorbance results improved after the PMMA and GO loading additive, respectively. At 320 nm^{-1}, the absorption for N1 appears to be 0.8 in the ultraviolet region, which significantly improved to 0.94 and 0.98 for N2 and N3, respectively, which the contribution of the PMMA and GO, respectively. The absorption for H1 was 0.71 and significantly increased to 0.83 and 0.97 for H2 and H3, respectively. Generally, the absorption results depicted notable development in the absorbance value up to 54% for N2, while enhancement to 132% after adding GO for N3. The nanocomposite exposed an outstanding improvement in the outcomes assessed to the nano/hybrid dental filling because the electrons

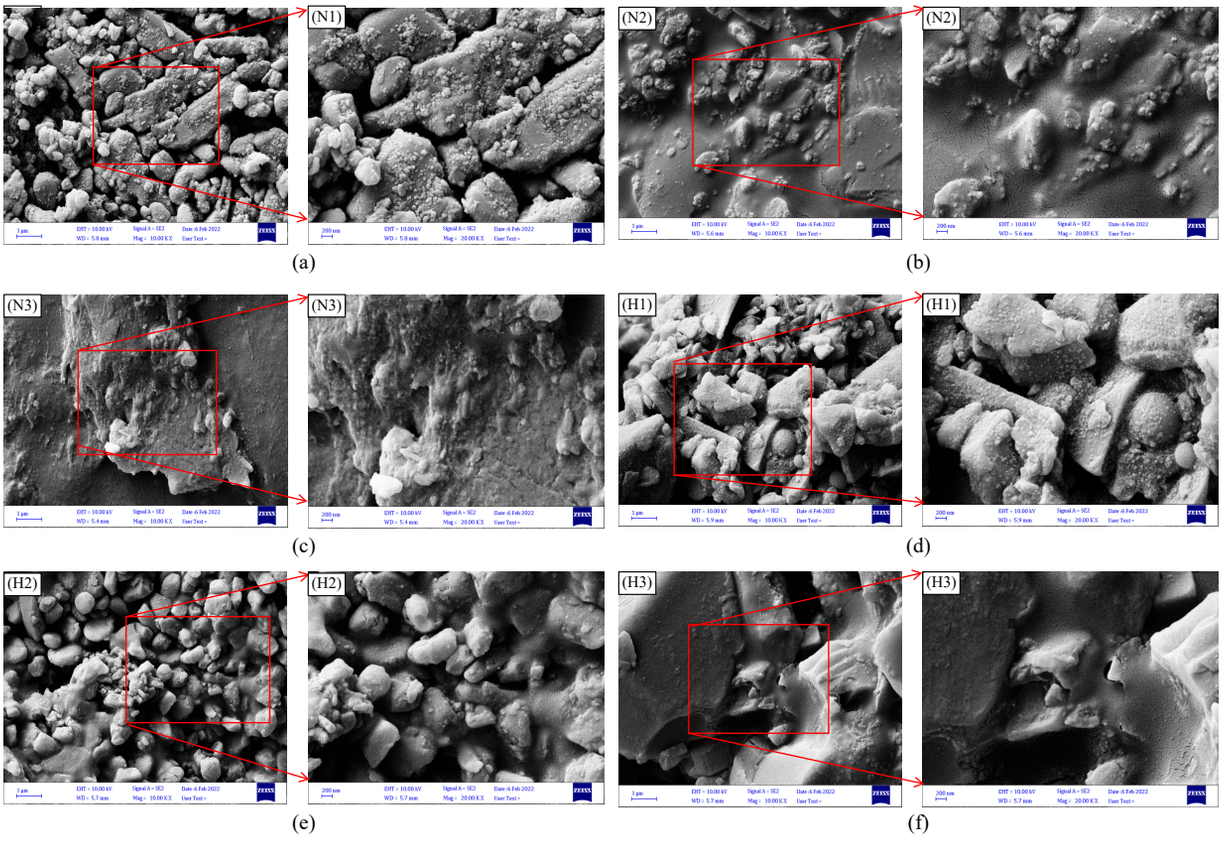

Fig. 3 SEM images with two magnifications micron (left column) and nano (right column) of the surface morphology of the samples **(a)** N1; **(b)** N2; **(c)** N3; **(d)** H1; **(e)** H2; **(f)** H3.

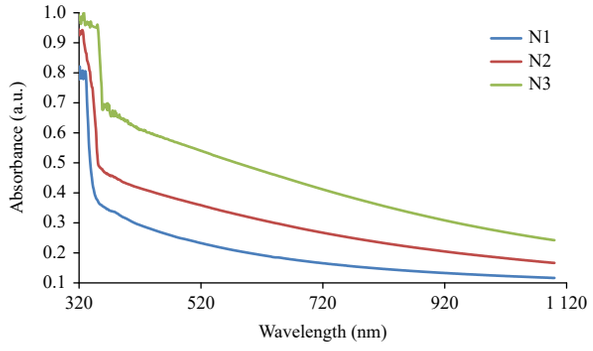

Fig. 4 Absorbance spectra for the N1, N2, and N3 nanocomposite film with the wavelength.

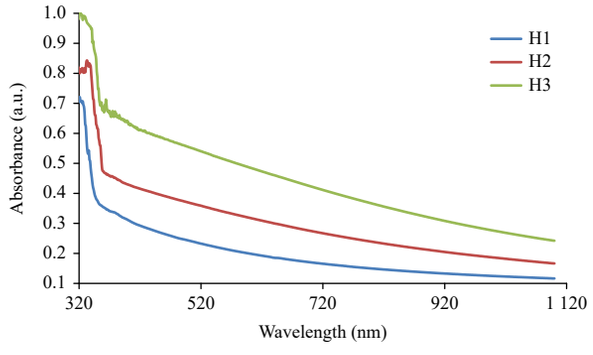

Fig. 5 Absorbance spectra for the H1, H2, and H3 nanocomposite film with wavelength.

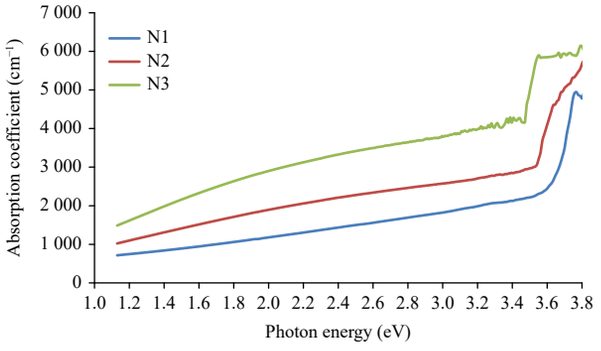

Fig. 6 Absorption coefficient for the N1, N2, and N3 nanocomposite with photon energy.

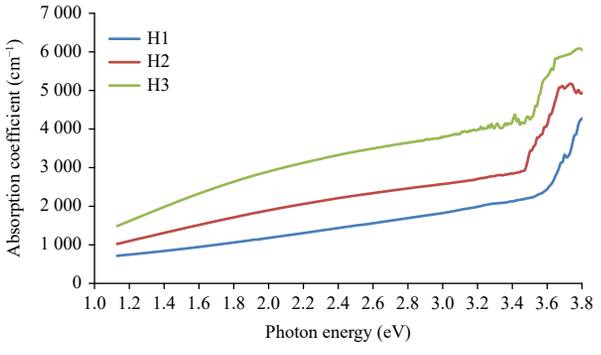

Fig. 7 Absorption coefficient for the H1, H2, and H3 nanocomposites with photon energy.

could absorb the incident light and electromagnetic energy and then transmit at higher energy levels [42].

The absorption coefficient (α) is provided as in Ref. [43]:

$$\alpha = 2.303 \times A/t \tag{1}$$

where A is the absorption and t is the thickness of the samples. Figures 6 and 7 illustrate the absorption coefficient vs. photon energy for the samples and nanocomposites. At the low energy, α was the smallest, attributed to the small probability of electron transition. The incident photon energy was not enough to transfer the electron of the valence band to the conduction band. In contrast, it was possible at higher energy, as presented in Figs. 6 and 7. The absorption coefficient results indicated a high probability of the indirect transition because its value was lower than 10^4 cm^{-1}.

The indirect energy gap is given by the following equation [21]:

$$(\alpha h\nu)^{1/m} = B(h\nu - E_g) \tag{2}$$

B, $h\nu$, and E_g mean constant, photon energy, and energy gap, respectively, whereas m equals 2 or 3 to the indirect transition of allowed and forbidden. Figures 8–11 demonstrate the absorption edge of allowed indirect transition and forbidden indirect transition for N1, N2, N3, and H1, H2, and H3 as a function of the photon energy. However, linear part intercept extrapolated was utilized to calculate these quantities at $(ahv)^{1/m} = 0$.

As shown in Table 2, the optical energy gap reduced as the concentration of PMMA and GO increased. This may be described as follows: Increasing molecular weight increases the degree of disorder. In addition, the photon energy absorption of incident light reveals which photon energies have been allocated to fracturing and partially bending the polymer crystalline structure. As the disorder level of a polymer increases, the estimated optical gap decreases [44].

The coefficient of extinction k is determined by Ref. [21]:

$$k = \frac{\alpha\lambda}{4\pi} \tag{3}$$

where λ means the wavelength. The extinction coefficients for N1, N2, N3, and H1, H2, and H3 nanocomposites as a function of wavelength are

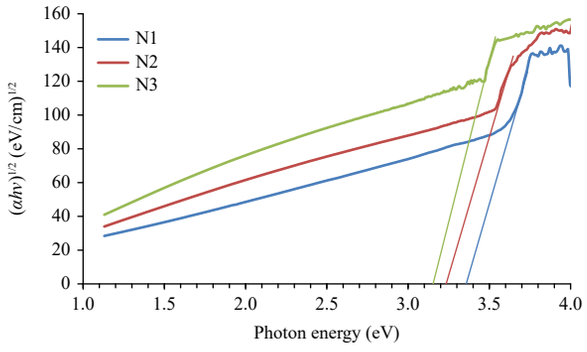

Fig. 8 E_g for the allowed indirect transition with the photon energy of samples.

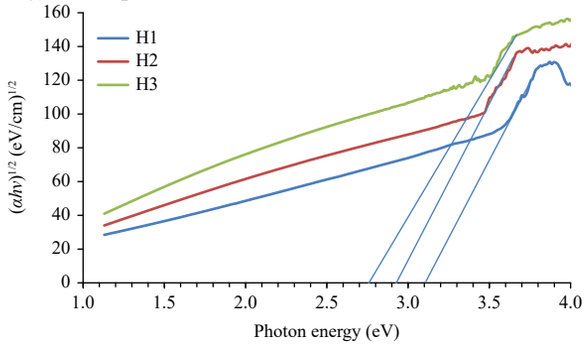

Fig. 9 E_g of the allowed indirect transition for the samples with the photon energy.

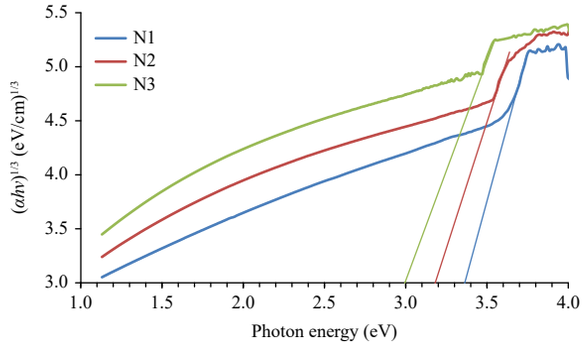

Fig. 10 E_g of the forbidden indirect transition for samples with the photon energy.

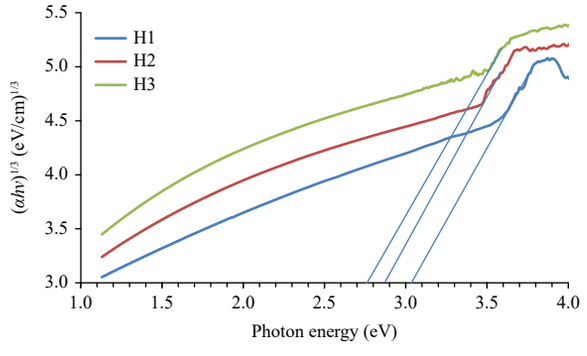

Fig. 11 E_g of the forbidden indirect transition for the samples with the photon energy.

Table 2 E_g for samples

Samples	Indirect transition (eV)	
	Allowed	Forbidden
N1	3.35	3.38
N2	3.25	3.2
N3	3.15	3
H1	3.10	3.05
H2	2.95	2.89
H3	2.75	2.75

individually displayed in Figs. 12 and 13. From these figures, it is observed that the value of the extinction coefficient was improved with the contribution of PMMA and GO nanosheets.

The equation below determines the refractive index (n) [45]:

$$n = \frac{1+\sqrt{R}}{1-\sqrt{R}} \tag{4}$$

where R is the reflectance.

Figures 14 and 15 demonstrate the variation refractive index for N1, N2, N3, and H1, H2, and H3 nanocomposite film versus wavelength individually.

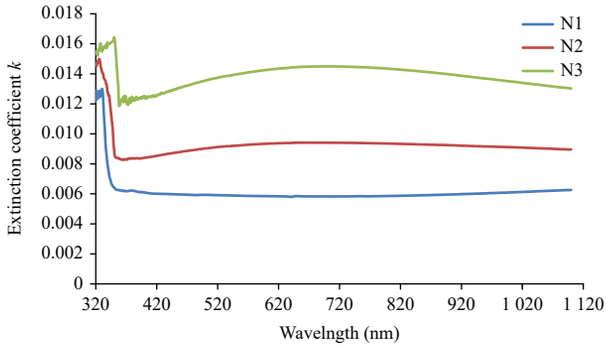

Fig. 12 The extinction coefficient for the N1, N2, and N3 nanocomposites vs. wavelength.

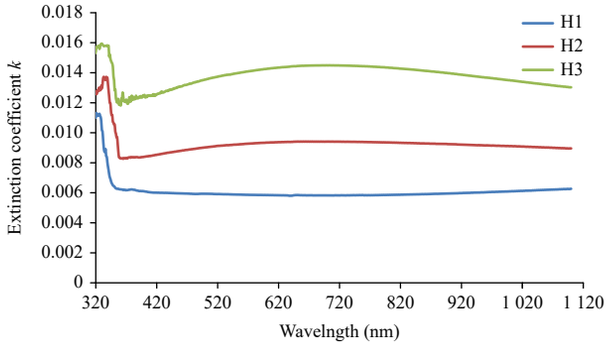

Fig. 13 Extinction coefficient for the H1, H2, and H3 nanocomposites vs. wavelength.

Figure 14 detected anomalous dispersion of the refractive index in the spectral $\lambda < 620$ nm, whereas it was normal dispersion in the range of > 620 nm. Figure 15 shows the anomalous dispersion at a wavelength of < 420 and normal dispersion $\lambda > 420$. This unusual behavior is a result of the resonance effect between the incident light and the electron's polarization, leading to the link of electrons in the nanocomposite to the oscillating electromagnetic field, followed by a rise in refractive index values with rising amounts of PMMA and GO in the dental filling and hybrid. This interpretation agrees with the results in Ref. [46].

The optical conductivity (σ_{op}) is defined by Ref [47]:

$$\sigma_{op} = \frac{\alpha nc}{4\pi} \quad (5)$$

where c means the velocity of light, Figures 16 and 17 illustrate the optical conductivity with wavelength for the N1, N2, N3, and H1, H2, and H3, respectively. It is noted that optical conductivity for all the samples rises with a rise in the PMMA and GO content. This behavior is related to a rise in the absorption and a reduction in the energy gap [48].

Antimicrobial agent is a phrase that refers to a chemical molecule that has the capability of destroying pathogenic microorganisms [49]. It is possible to include antibacterial filler particles into resin composite materials by modifying the filler particles themselves [50] or the resin mixture [51]. *Klebsiella* is a genus of Gram-negative bacteria, a member of the family Enterobacteriaceae, a non-motile, spore-forming, rod-shaped bacterium with a prominent capsule composed of polysaccharides. It causes pneumonia, urinary infection, and septicemia [52].

A McFarland 0.5 turbidity standard was prepared adding 99.5 mL of 1% sulfuric acid to 0.5 mL of 1.175% barium chloride solution. This solution was dispensed into tubes comparable to those used for inoculum preparation. The tubes were sealed and stored under dark conditions room temperature. The McFarland standard provided turbidity comparable to that of a bacterial suspension containing 1.5 × 10 cells/μL. The turbidity of the prepared bacterial suspensions was compared by observing the black lines through the suspension [53]. The results, depicted in Fig. 18, demonstrated that the samples

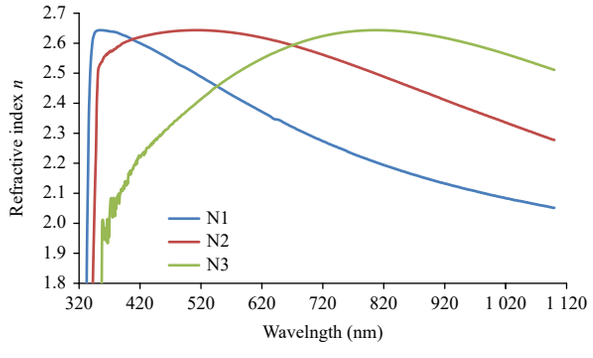

Fig. 14 Refractive index for the N1, N2, and N3 nanocomposites vs. wavelength.

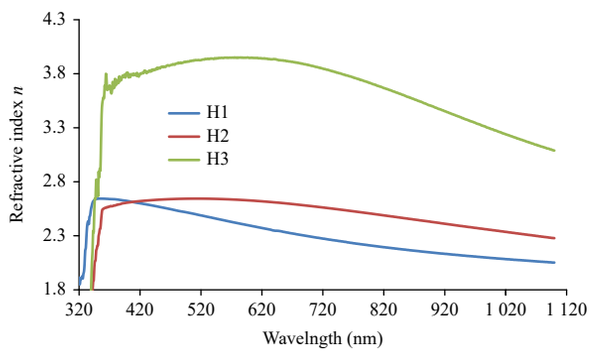

Fig. 15 Refractive index for the H1, H2, and H3 nanocomposite film vs. wavelength.

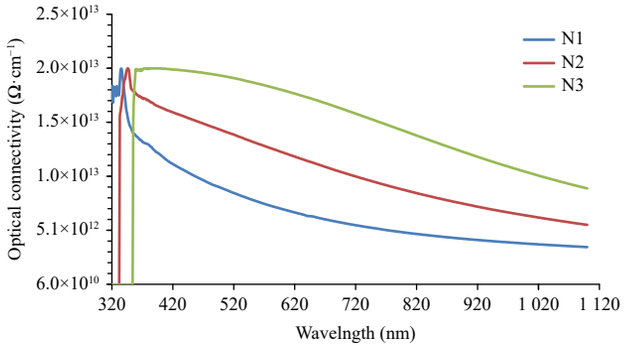

Fig. 16 Optical conductivity for the N1, N2, and N3 nanocomposites vs. wavelength.

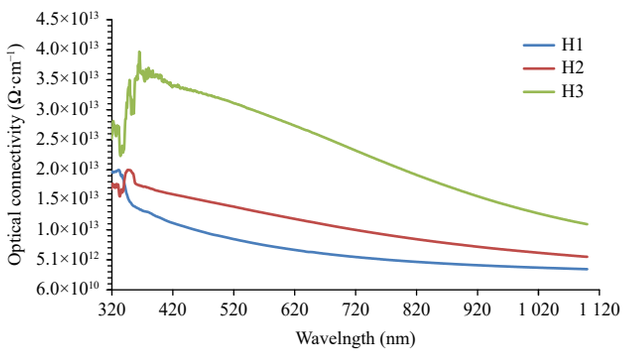

Fig. 17 Optical conductivity for the H1, H2, and H3 nanocomposites vs. wavelength.

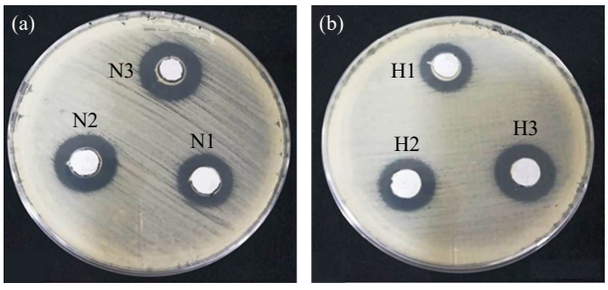

Fig. 18 *In vitro* antibacterial activity of dental filler samples against *Klebsiella*.

Table 3 Zone of inhibition of antibacterial generated dental filler samples

Zone of inhibition (mm)	
Bacterial isolates	*Klebsiella*
N1	17
N2	19
N3	23
H1	16
H2	18.5
H3	22

successfully combat the *Klebsiella* bacteria. The nano dental filling (N1) showed resistance to bacteria with an inhibitory zone of 17 mm in diameter against *Klebsiella*. This value slightly increased to 19 mm after including PMMA in N2. As shown in Table 3, adding GO in N3 led to a considerable zone expansion in which *Klebsiella* could no longer grow. The hybrid dental filling (H1) was shown to be resistant to germs, and the zone of inhibition diameter against *Klebsiella* was discovered to be 16 mm. The addition of PMMA to H2 increased the diameter of the zone of inhibition against *Klebsiella* from 16 to 18.5 mm. It's showed that H3 (with GO) was more effective than H1, which led to a considerable improvement in the zone of inhibition against *Klebsiella*, up to 22 mm as shown in Table 3.

Whereas dental fillings made of nano and hybrid materials are resistant to germs. After adding the PMMA, there was a minor rise in this resistance; however, after adding the nanosheets (GO), the killing area has a definite increase. It noted that cells entrapment could be an additional plausible mechanism behind the antibacterial effects of GO. When the bacterial cells meet the GO sheets, the sheets may develop the ability to trap the cells. GO is able to destroy the imprisoned bacteria, cutting off the outer microenvironment, thus their access to nutrition elements will be reduced, resulting in hindering bacterial growth. The size of the GO may have a significant impact on the encapsulation of the cells in this setting [54, 55].

Generally, PMMA nano/hybrid filler-GO dental samples showed a better ability to kill the bacteria and a more extensive zone of inhibition diameter of antibacterial.

Conclusion

The procedure effectively prepared the PMMA-nano/hybrid filler-GO dental nanocomposite fillers. The FTIR result confirmed the functional groups of each component and the strong impact and good interaction among the fillers, PMMA, and reinforcement GO nanosheets. The images of the OPM exposed a homogeneous surface and good dispersion of nanomaterials. SEM images showed the changes in the morphology after the contribution of PMMA and GO nanosheets. The findings exposed the critical impact of PMMA and GO nanosheets on the optical properties of nano and hybrid-dental nanocomposite fillers compared with original fillers. This is evident in the increases values of the absorbance: up to 54% for N2, up to 132% for N3. The energy gap reduces with increased additive PMMA and GO. The optical properties, and optical conductivity for all the samples significantly improved with increasing the matrix's PMMA and GO loading content. These results highlight promising new modified fillers in this study that could be cheaper and stronger with the most extended lifetime than the original dental fillers, which could easily be used and change the filler's future. Generally, nanofiller dental samples showed a better ability to kill the bacteria: N3, the zone of inhibition diameter, increased from 17 to 23 mm for nano-filling and from 16 to 22 mm for hybrid-filling.

CRediT Author Statement

Abbas Kadhim Hassan: investigation, acquisition, formal analysis, data curation, and writing the original draft. **Habib Hamidinezhad** and **Ehssan Al-Bermany:** Validation, project administration, investigation, resources, review, and editing.

Acknowledgements

The authors gratefully acknowledge M.S.E. from the University of Sheffield, UK and Composite Nanomaterials group from the Department of Physics, the University of Babylon, Iraq for their support.

Conflict of Interests

The authors declare that they have no conflict of interest.

Supporting Information

Supporting information to this article can be found online at http://doi.org/10.26599/NBE.2024.9290075.

References

[1] A. Bregnocchi, E. Zanni, D. Uccelletti, et al. Graphene-based dental adhesive with anti-biofilm activity. *Journal of Nanobiotechnology*, 2017, 15(1): 89. https://doi.org/10.1186/s12951-017-0322-1

[2] E. Al-Bermany, B.Q. Chen. Preparation and characterisation of poly(ethylene glycol)-adsorbed graphene oxide nanosheets. *Polymer International*, 2021, 70(3): 341−351. https://doi.org/10.1002/pi.6140

[3] N. Beyth, A.J. Domb, E.I. Weiss. An *in vitro* quantitative antibacterial analysis of amalgam and composite resins. *Journal of Dentistry*, 2007, 35(3): 201−206. https://doi.org/10.1016/j.jdent.2006.07.009

[4] K. Abdali, K.H. Abass, E. Al-Bermany, et al. Morphological, optical, electrical characterizations and anti- escherichia coli bacterial efficiency (AECBE) of PVA/PAAm/PEO polymer blend doped with silver NPs;. *Nano Biomedicine and Engineering*, 2022, 14(2): 114−122. https://doi.org/10.5101/nbe.v14i2.p114-122

[5] J.L. Ferracane, T.J. Hilton. Polymerization stress–Is it clinically meaningful. *Dental Materials*, 2016, 32(1): 1−10. https://doi.org/10.1016/j.dental.2015.06.020

[6] A.R. Yadav, S.K. Mohite, C.S. Magdum. Preparation and evaluation of antibacterial herbal mouthwash against oral pathogens. *Asian Journal of Research in Pharmaceutical Science*, 2020, 10(3): 149. https://doi.org/10.5958/2231-5659.2020.00028.4

[7] K.H. Metwalli, S.A. Khan, B.P. Krom, et al. *Streptococcus mutans*, *Candida albicans*, and the human mouth: A sticky situation. *PLoS Pathogens*, 2013, 9(10): e1003616. https://doi.org/10.1371/journal.ppat.1003616

[8] M. Nayak. Effect of modern (junk) food in dental caries. *Indian Journal of Forensic Medicine & Toxicology*, 2020, 14(4): 9194−9197. https://doi.org/10.37506/ijfmt.v14i4.13183

[9] L. Cheng, K. Zhang, M.D. Weir, et al. Nanotechnology strategies for antibacterial and remineralizing composites and adhesives to tackle dental caries. *Nanomedicine*, 2015, 10(4): 627−641. https://doi.org/10.2217/nnm.14.191

[10] V. Kassardjian, M. Andiappan, N.H.J. Creugers, et al. A systematic review of interventions after restoring the occluding surfaces of anterior and posterior teeth that are affected by tooth wear with filled resin composites. *Journal of Dentistry*, 2020, 99: 103388. https://doi.org/10.1016/j.jdent.2020.103388

[11] A.N. Al-Jamal, O. Karar Abdali, K.H. Abbass, et al. Silver NPs reinforced the structural and mechanical properties of PVA-PAAm-PEG nanocomposites. *AIP Conference Proceedings*, 2023, 2414: 030005. https://doi.org/10.1063/5.0114621

[12] N. Beyth, S. Farah, A.J. Domb, et al. Antibacterial dental resin composites. *Reactive and Functional Polymers*, 2014, 75: 81−88. https://doi.org/10.1016/j.reactfunctpolym.2013.11.011

[13] K. Abdali, B.H. Rabee, E. Al-Bermany, et al. Effect of doping Sb_2O_3NPs on morphological, mechanical, and dielectric properties of PVA/PVP blend film for electromechanical applications. *Nano*, 2023, 18(3): 2350011. https://doi.org/10.1142/s179329202350011x

[14] Z.Y. Ge, L.M. Yang, F. Xiao, et al. Graphene family nanomaterials: Properties and potential applications in dentistry. *International Journal of Biomaterials*, 2018, 2018: 1539678. https://doi.org/10.1155/2018/1539678

[15] A.A. Fadhl Abodood, K. Abdali, A.O. Mousa Al-Ogaili, et al. Effect of molar concentration and solvent type on linear and NLO properties of aurintricarboxylic (ATA) organic dye for image sensor and optical limiter applications. *International Journal of Nanoscience*, 2023, 22(2): 2350014. https://doi.org/10.1142/s0219581x2350014x

[16] W. Hu, C. Peng, W. Luo, et al. Graphene-based antibacterial paper. ACS Nano 2010, 4(7): 4317–4323.

[17] M.F. Şuhani, G. Băciuţ, M. Băciuţ, et al. Current perspectives regarding the application and incorporation of silver nanoparticles into dental biomaterials. *Clujul Medical* (*1957*), 2018, 91(3): 274–279. https://doi.org/10.15386/CJMED-935

[18] S. Imazato, S. Ma, J.H. Chen, et al. Therapeutic polymers for dental adhesives: Loading resins with bio-active components. *Dental Materials*, 2014, 30(1): 97−104. https://doi.org/10.1016/j.dental.2013.06.003

[19] A.N. Obaid, E. Al-Bermany. Performance of functionalized graphene oxide to improve anti-corrosion of epoxy coating on 2024-T3 aluminium alloy. *Materials Chemistry and Physics*, 2023, 305: 127849. https://doi.org/10.1016/j.matchemphys.2023.127849

[20] A.J. Al-bermany, R.A.-A. Ghazi. Study the effect of increasing Gamma ray doses on some physical properties of Carboxy methyl cellulose. *Advances in Physics Theories and Applications*, 2012, 6: 1−14.

[21] K. Abdali, E. Al-Bermany, K.H. Abass. Impact the silver nanoparticles on properties of new fabricated polyvinyl alcohol- polyacrylamide- polyacrylic acid nanocomposites films for optoelectronics and radiation pollution applications. *Journal of Polymer Research*, 2023, 30(4): 138. https://doi.org/10.1007/s10965-023-03514-y

[22] A.K. Al-shammari, E. Al-Bermany. Polymer functional group impact on the thermo-mechanical properties of polyacrylic acid, polyacrylic amide- poly (vinyl alcohol) nanocomposites reinforced by graphene oxide nanosheets. *Journal of Polymer Research*, 2022, 29(8): 351. https://doi.org/10.1007/s10965-022-03210-3

[23] S.H. Al-Nesrawya, M.J. Mohseenb, E. Al-Bermany. Reinforcement the mechanical properties of (NR50/SBRs50/OSP) composites with oyster shell powder and carbon black. *IOP Conference Series*:

Materials Science and Engineering, 2020, 871: 012060. https://doi.org/10.1088/1757-899X/871/1/012060

[24] M. Abdul kadhim, E. Al-bermany. Enhance the electrical properties of the novel fabricated PMMA-PVA/graphene based nanocomposites. *Journal of Green Engineering*, 2020, 10(7): 3465−3483.

[25] S. Khindria, S. Mittal, U. Sukhija. Evolution of denture base materials. *The Journal of Indian Prosthodontic Society*, 2009, 9(2): 64−69. https://doi.org/10.4103/0972-4052.55246

[26] A.I. Abdelamir, E. Al-Bermany, F. Sh Hashim. Enhance the optical properties of the synthesis PEG/graphene-based nanocomposite films using GO nanosheets. *Journal of Physics*: *Conference Series*, 2019, 1294(2): 022029. https://doi.org/10.1088/1742-6596/1294/2/022029

[27] A.R. Torabi, S. Shahbaz, S. Cicero, et al. Fracture testing and estimation of critical loads in a PMMA-based dental material with nonlinear behavior in the presence of notches. *Theoretical and Applied Fracture Mechanics*, 2022, 118: 103282. https://doi.org/10.1016/j.tafmec.2022.103282

[28] K.D. Jandt, D.C. Watts. Nanotechnology in dentistry: Present and future perspectives on dental nanomaterials. *Dental Materials*, 2020, 36(11): 1365−1378. https://doi.org/10.1016/j.dental.2020.08.006

[29] G.C. Padovani, V.P. Feitosa, S. Sauro, et al. Advances in dental materials through nanotechnology: Facts, perspectives and toxicological aspects. *Trends in Biotechnology*, 2015, 33(11): 621−636. https://doi.org/10.1016/j.tibtech.2015.09.005

[30] S.A. Jasim, H.A.J. Banimuslem, F.H. Alsultany, et al. Ammonia and nitrogen dioxide detection using ZnO/CNT nanocomposite synthesized by sol–gel technique. *Journal of Sol-Gel Science and Technology*, 2023, 108(3): 734−741. https://doi.org/10.1007/s10971-023-06190-y

[31] N.R. Aldulaimi, E. Al-Bermany. Tuning the bandgap and absorption behaviour of the newly-fabricated ultrahigh molecular weight polyethylene oxide-polyvinyl alcohol/graphene oxide hybrid nanocomposites. *Polymers and Polymer Composites*, 2022, 30. https://doi.org/10.1177/09673911221112196

[32] A. Radhi, D. Mohamad, F.S. Abdul Rahman, et al. Mechanism and factors influence of graphene-based nanomaterials antimicrobial activities and application in dentistry. *Journal of Materials Research and Technology*, 2021, 11: 1290−1307. https://doi.org/10.1016/j.jmrt.2021.01.093

[33] E. Al-Bermany, D. Qais, S. Al-Rubaye. Graphene effect on the mechanical properties of poly (ethylene oxide)/graphene oxide nanocomposites using ultrasound technique. *Journal of Physics*: *Conference Series*, 2019, 1234(1): 012011. https://doi.org/10.1088/1742-6596/1234/1/012011

[34] E. Al-Bermany, A.T. Mekhalif, H.A. Banimuslem, et al. Effect of green synthesis bimetallic Ag@SiO_2 core–shell nanoparticles on absorption behavior and electrical properties of PVA-PEO nanocomposites for optoelectronic applications. *Silicon*, 2023, 15(9): 4095−4107. https://doi.org/10.1007/s12633-023-02332-7

[35] C. Bacali, R. Carpa, S. Buduru, et al. Association of graphene silver polymethyl methacrylate (PMMA) with photodynamic therapy for inactivation of halitosis responsible bacteria in denture wearers. *Nanomaterials*, 2021, 11(7): 1643. https://doi.org/10.3390/nano11071643

[36] S. Malik, F.M. Ruddock, A.H. Dowling, et al. Graphene composites with dental and biomedical applicability. *Beilstein Journal of Nanotechnology*, 2018, 9: 801−808. https://doi.org/10.3762/bjnano.9.73

[37] M.T.H. Aunkor, T. Raihan, S.H. Prodhan, et al. Antibacterial activity of graphene oxide nanosheet against multidrug resistant superbugs isolated from infected patients. *Royal Society Open Science*, 2020, 7(7): 200640. https://doi.org/10.1098/rsos.200640

[38] D. Ali Hameed, N. Ameer. Nano silica and nano graphene used in dental fillers: The relation between the mechanical and topography properties. *Research Journal of Medical Sciences*, 2020, 14(1): 20−25. https://doi.org/10.36478/rjmsci.2020.20.25

[39] W.S. Jr. Hummers, R.E. Offeman. Preparation of graphitic oxide. *Journal of the American Chemical Society*, 1958, 80(6): 1339. https://doi.org/10.1021/ja01539a017

[40] M.A. Kadhim, E. Al-Bermany. New fabricated PMMA-PVA/graphene oxide nanocomposites: Structure, optical properties and application. *Journal of Composite Materials*, 2021, 55(20): 2793−2806. https://doi.org/10.1177/0021998321995912

[41] E. Al-Bermany, B.Q. Chen. Effect of the functional groups of polymers on their adsorption behavior on graphene oxide nanosheets. *Macromolecular Chemistry and Physics*, 2023, 224(16): 2300101. https://doi.org/10.1002/macp.202300101

[42] S. Villar-Rodil, J.I. Paredes, A. Martínez-Alonso, et al. Preparation of graphene dispersions and graphene-polymer composites in organic media. *Journal of Materials Chemistry*, 2009, 19(22): 3591. https://doi.org/10.1039/b904935e

[43] Micozzi, M.S., Townsend, F.M., Koop, C.E. From Army Medical Museum to National Museum of Health and Medicine. A century-old institution on the move. *Archives of Pathology & Laboratory Medicine*, 1990, 114: 1290−1295.

[44] K.A.M. Abd El-Kader, S.F. Abdel Hamied, A.B. Mansour, et al. Effect of the molecular weights on the optical and mechanical properties of poly(vinyl alcohol) films. *Polymer Testing*, 2002, 21(7): 847−850. https://doi.org/10.1016/S0142-9418(02)00020-X

[45] V.N. Suryawanshi, A.S. Varpe, M.D. Deshpande. Band gap engineering in PbO nanostructured thin films by Mn doping. *Thin Solid Films*, 2018, 645: 87−92. https://doi.org/10.1016/j.tsf.2017.10.016

[46] Salloom, H.T., Jasim, A.S., Hamad, T.K. Synthesis and optical characterization of Ag/PVA nanocomposites films. Journal of Al-Nahrain University, 2017, 20(4): 56–63. https://doi.org/10.22401/jnus.20.4.10

[47] A. Hazim, A. Hashim, H. Abduljalil. Fabrication of novel (PMMA-Al_2O_3/Ag) nanocomposites and its structural and optical properties for lightweight and low cost electronics applications. *Egyptian Journal of Chemistry*, 2021, 64(1): 359−374.

[48] S.A. Jabbar, S.M. Khalil, A.R. Abdulridha, et al. Dielectric, AC conductivity and optical characterizations of (PVA-PEG) doped SrO hybrid nanocomposites. *Key Engineering Materials*, 2022, 936: 83−92. https://doi.org/10.4028/p-41a757

[49] E.R. Kenawy, S.A. Khattab, M.M. Azaam. Synthesis and antibacterial activity of schiff base compounds based on poloxamine. *Delta Journal of Science*, 2019, 40(1): 69−77. https://doi.org/10.21608/djs.2019.139205

[50] N.L. Sánchez Vásquez. Control de la placa dental en pacientes con ortodoncia. Una revisión de la literatura. *Kiru*, 2019, 16(2): 92−96. https://doi.org/10.24265/kiru.2019.v16n2.06

[51] W. Zhou, X. Peng, X.D. Zhou, et al. *In vitro* evaluation of

composite containing DMAHDM and calcium phosphate nanoparticles on recurrent caries inhibition at bovine enamel-restoration margins. *Dental Materials*, 2020, 36(10): 1343–1355. https://doi.org/10.1016/j.dental.2020.07.007

[52] E. Denkovskienė, Š. Paškevičius, A. Misiūnas, et al. Broad and efficient control of klebsiella pathogens by peptidoglycan-degrading and pore-forming bacteriocins klebicins. *Scientific Reports*, 2019, 9: 15422. https://doi.org/10.1038/s41598-019-51969-1

[53] T.C. Goh, M.Y. Bajuri, S. C Nadarajah, et al. Clinical and bacteriological profile of diabetic foot infections in a tertiary care. *Journal of Foot and Ankle Research*, 2020, 13(1): 36. https://doi.org/10.1186/s13047-020-00406-y

[54] S.B. Liu, M. Hu, T.H. Zeng, et al. Lateral dimension-dependent antibacterial activity of graphene oxide sheets. *Langmuir*, 2012, 28(33): 12364−12372. https://doi.org/10.1021/la3023908

[55] A.I. Alawi, E. Al-Bermany. Newly fabricated ternary PAAm-PVA-PVP blend polymer doped by SiO_2: Absorption and dielectric characteristics for solar cell applications and antibacterial activity. *Silicon*, 2023, 15(13): 5773−5789. https://doi.org/10.1007/s12633-023-02477-5